Isolation and functional characterization of a methyl jasmonate-responsive 3-carene synthase from *Lavandula x intermedia*

Ayelign M. Adal, Lukman S. Sarker, Ashley D. Lemke and Soheil S. Mahmoud*

Department of Biology, University of British Columbia, 1177 Research Rd, Kelowna, BC. V1V 1V7, Canada
*Corresponding author e-mail: soheil.mahmoud@ubc.ca

Abstract

Key message A methyl jasmonate responsive *3-carene synthase (Li3CARS)* gene was isolated from *Lavandula x intermedia* and functionally characterized *in vitro*.

Lavenders produce essential oils consisting mainly of monoterpenes, including the potent antimicrobial and insecticidal monoterpene 3-carene. In this study we isolated and functionally characterized a leaf-specific, methyl jasmonate (MeJA)-responsive monoterpene synthase (Li3CARS) from *Lavandula x intermedia.* The ORF excluding transit peptides encoded a 64.9 kDa protein that was expressed in *E. coli,* and purified with Ni-NTA agarose affinity chromatography. The recombinant Li3CARS converted GPP into 3-carene as the major product, with K_m and k_{cat} of 3.69 ± 1.17 µM and 2.01 s^{-1} respectively. Li3CARS also accepted NPP as a substrate to produce multiple products including a small amount of 3-carene. The catalytic efficiency of Li3CARS to produce 3-carene was over 10 fold higher for GPP (k_{cat}/K_m = 0.56 $\mu M^{-1}s^{-1}$) than NPP (k_{cat}/K_m = 0.044 $\mu M^{-1}s^{-1}$). Production of distinct end product profiles from different substrates (GPP versus NPP) by Li3CARS indicates that monoterpene metabolism may be controlled in part through substrate availability. *Li3CARS* transcripts were found to be highly abundant in leaves (16 fold) as compared to flower tissues. The transcriptional activity of *Li3CARS* correlated with 3-carene production, and was up-regulated (1.18 - 3.8 fold) with MeJA 8 - 72 h post-treatment. The results suggest that *Li3CARS* may have a defensive role in *Lavandula*.

Key words: 3-carene synthase, *Lavandula*, *Lavandula x intermedia*, methyl jasmonate, monoterpene synthase, transcriptional regulation

Abbreviations: BPPS- bornyl pyrophosphate synthase; EO- essential oil; GPP- geranyl pyrophosphate; MeJA- methyl jasmonate; mTPS- monoterpene synthase; Li3CARS- *L. x intermedia* 3-carene synthase; NPP- neryl pyrophosphate; qPCR- quantitative real-time PCR; TPS- terpene synthase

Key Message

A methyl jasmonate responsive *3-carene synthase (Li3CARS)* gene was isolated from *Lavandula x intermedia* and functionally characterized *in vitro*. The recombinant Li3CARS catalyzed conversion of GPP to 3-carene as the main product. The genome organization, evolutionary relationship, homology-based modeling and differential expression of Li3CARS are discussed.

Isolation and functional characterization of a methyl jasmonate-responsive 3-carene synthase from *Lavandula x intermedia*

Abstract

Lavenders produce essential oils consisting mainly of monoterpenes, including the potent antimicrobial and insecticidal monoterpene 3-carene. In this study we isolated and functionally characterized a leaf-specific, methyl jasmonate (MeJA)-responsive monoterpene synthase (Li3CARS) from *Lavandula x intermedia.* The ORF excluding transit peptides encoded a 64.9 kDa protein that was expressed in *E. coli,* and purified with Ni-NTA agarose affinity chromatography. The recombinant Li3CARS converted GPP into 3-carene as the major product, with K_m and k_{cat} of 3.69 ± 1.17 µM and 2.01 s^{-1} respectively. Li3CARS also accepted NPP as a substrate to produce multiple products including a small amount of 3-carene. The catalytic efficiency of Li3CARS to produce 3-carene was over 10 fold higher for GPP (k_{cat}/K_m = 0.56 $\mu M^{-1}s^{-1}$) than for NPP (k_{cat}/K_m = 0.044 $\mu M^{-1}s^{-1}$). Production of distinct end product profiles from different substrates (GPP versus NPP) by Li3CARS indicates that monoterpene metabolism may be controlled in part through substrate availability. *Li3CARS* transcripts were found to be highly abundant in leaves (16 fold) as compared to flower tissues. The transcriptional activity of *Li3CARS* correlated with 3-carene production, and was up-regulated (1.18 - 3.8 fold) with MeJA 8 - 72 h post-treatment. The results suggest that *Li3CARS* may have a defensive role in *Lavandula*.

Isolation and functional characterization of a methyl jasmonate-responsive 3-carene synthase from *Lavandula x intermedia*

Introduction

Plants produce a large assortment of isoprenoids - the largest class of specialized metabolites-, some of which serve important physiological function, for example as growth regulators (e.g. gibberellins, abscisic acid and brassinolide) and constitutes of the photosynthetic machinery (e.g. carotenoids) (Tholl and Lee 2011). Several isoprenoids play ecological roles, facilitating interactions of plants with their environment, acting for example in attracting pollinators, providing defenses and priming the neighbor plants (Frost et al. 2007; Menzel et al. 2014; De Vega et al. 2014). In many plants, isoprenoids have been found to have direct defensive roles, for example as phytoalexins, against microbes and herbivores, and indirect defensive functions as attractors of enemy predators and parasitoids (Fäldt et al. 2003; Hasegawa et al. 2010; Heiling et al. 2010; Menzel et al. 2014). Certain isoprenoids may also be involved in plants protection against abiotic stresses, such as exposure to high temperature, and reactive oxygen species-derived oxidative damages (Vickers et al. 2009).

The biosynthesis of isoprenoids begins with synthesis of the common C_5 isoprene units- isopentenyl pyrophosphate (IPP) and dimethylallyl pyrophosphate (DMAPP)- through the plastidial 2-C- methyl- D- erythritol- 4- phosphate (MEP) and cytosolic mevalonate (MVA) pathways (Tholl and Lee 2011; Dudareva et al. 2013). IPP and DMAPP are then condensed head-to-tail by specific pernyltransferases to produce linear precursors of most isoprenoids, such as C_{10} geranyl pyrophosphate (GPP), C_{10} neryl pyrophosphate (NPP) and C_{15} farnesyl pyrophosphate (FPP) (Burke et al. 1999; Schilmiller et al. 2009; Tholl and Lee 2011). The head-to-middle coupling of the two DMAPP can also be catalyzed by a distinct class of pernyltransferases exemplified by lavandulyl pyrophosphate synthase and chrysanthemyl diphosphate synthase, which synthesize the irregular C_{10} terpene precursors lavandulyl pyrophosphate (LPP) (Demissie et al. 2013) and C_{10} chrysanthemyl diphosphate (CPP) (Rivera et al. 2001), respectively. The linear precursors are then transformed into various isoprenoids by specific synthases, collectively known as terpene synthases (TPSs) (Tholl and Lee 2011). Further modifications of the terpene skeletons are also possible through the action of enzymes such as acetyltransferases, P450 hydroxylases, and so on (Fig. 1).

The biosynthesis of isoprenoids - and hence the expression of TPSs - can be triggered by several factors including herbivores and microbial attacks, phytohormones and other elicitors. For instance, direct herbivore attack and pathogen infection activates the transcriptional expression of some mono- and sesquiterpene synthases in Arabidopsis, Sitka spruce, Norway spruce, maize and lima bean (Fäldt et al. 2003; Miller et al. 2005; Navia-Giné et al. 2009; Huang et al. 2010; Fontana et al. 2011). Further, these genes can be induced by exogenous phytohormones and elicitors such as gibberellic acid, methyl jasmonate, salicylic acid and wounding (Van Schie et al. 2007; Heiling et al. 2010; Menzel et al. 2014; Taniguchi et al. 2014).

Several species of *Lavandula* (*Lamiaceae)* produce essential oils (EOs) that are composed of mono- and – to a lesser extent - sesquiterpenes. Although the specific isoprenoids involved in *Lavandula* defensive mechanisms in response to various pests remain unknown, the EOs and aqueous extracts from various lavender species have been reported to exhibit *in vitro* antimicrobial and insecticidal activities (Moon et al. 2006; De Rapper et al. 2013; Erland et al. 2015). The constitutive and induced isoprenoids play key roles in defense against important pests in different plants, such as in rice, tomato, maize and Arabidopsis (Wittstock and Gershenzon 2002; Van Schie et al. 2007; Huang et al. 2010; Fontana et al. 2011; Taniguchi et al. 2014), as well as in various coniferous plants (Miller et al. 2005; Boone et al. 2011; Ott et al. 2011; Byun-McKay et al. 2012). For example, 3-carene has been reported as a major induced defensive cyclic monoterpene in Lodgepole pine and Norway spruce trees (Fäldt et al. 2003; Byun-McKay et al. 2012), in which its accumulation positively correlates with plant resistance to white weevil (Robert et al. 2010). Thus, identifying specific monoterpenes and their respective synthase genes that contribute potentially to defensive strategies of *Lavandula* would be useful for the development of tolerant/resistant cultivars of lavenders.

To benefit *Lavandula* from the recent advances of molecular tools, our group has developed EST databases derived from different tissues of two economically important species, *L. angustifolia* and *L. x intermedia* (Lane et al. 2010; Demissie et al. 2012; Sarker et al. 2012). These tissue-specific EST databases have been instrumental in the identification of *TPS* genes in lavenders. Thus, using homology-based cloning, this study aimed to (1) clone and functionally characterize cDNA of a 3-carene synthase (*Li3CARS*) from *L. x intermedia,* and (2) study the expression pattern of the cloned gene in various settings. Here, we report the cloning of the *Li3CARS* cDNA, which was expressed and functionally characterized in *E. coli*. The recombinant Li3CARS catalyzed conversion of GPP to mainly 3-carene and few other minor products. The homology-based modeling of the Li3CARS protein helped in identifying the active site cavity and residues presumably involved in catalytic activities. Finally, the expression pattern of the *Li3CARS* in *L. x intermedia* plants was examined. The expression of this gene is induced by MeJA, suggesting that the *Li3CARS* may play a defensive role in lavenders.

Materials and methods

Plant growth and chemicals

L. x intermedia (cv. Grosso) plants were propagated by cuttings and were grown in potting Pro-Mix HP in a growth room maintained at 25°C under a 16/8 h light and dark photoperiod (approximately 200 µmol $m^{-2}s^{-1}$ of light, generated by cool-white fluorescent bulbs). The plants were watered every other day with addition of fertilizer (Miracle-Gro Fertilizers) once a week. Authentic isoprenoid standards and substrates for enzyme assays, including geranyl pyrophosphate (GPP), neryl pyrophosphate (NPP) and farnesyl pyrophosphate (FPP) were purchased from Sigma (http://www.sigmaaldrich.com/) and Echelon Biosciences (http://www.echelon-inc.com/), respectively. Unless otherwise mentioned, all other assay chemicals were obtained from Sigma.

Cloning of cDNA and genomic DNA

To clone the full-length cDNA, homology-based screening of mTPS from *L. x intermedia* EST library was done based on the sequences of *L. angustifolia* limonene synthase and *S. officinalis* bornyl pyrophosphate synthase genes, and selected cDNA clone was used for Sanger sequencing. The generated full-length sequence (Accession no: KX024762) was analyzed for potential targeting sequences using TargetP 1.1 (http://www.cbs.dtu.dk/services/TargetP/) and ChloroP 1.1 (http://www.cbs.dtu.dk/services/ChloroP/), and found to encode a chloroplast transit peptide at the N-terminus. For heterologous expression in *E. coli*, the putative N-terminal transit peptide was removed prior to designing the gene-specific cloning primer set. All primers used in this study are listed in Table 1. The open reading frame (ORF), excluding the transit peptide and stop codon, was cloned into the *Nde*I/*Kpn*I sites of pET41b(+) by sticky-end cloning (Zeng 1998).

Using appropriate primers the full-length genomic DNA for Li3CARS (Accession no.: KX024761) was amplified from *L. x intermedia* cloned into pGEM-T-Easy (Promega), and sequenced by Sanger sequencing.

Genome organization and phylogenetic analysis

Genomic organization of *Li3CARS* from *L. x intermedia* was predicted using the NCBI Spidey genomic DNA-mRNA aligner (http://www.ncbi.nlm.nih.gov/IEB/Research/Ostell/Spidey/spideyweb.cgi), targeting introns-exons number and size as well as intron position in the sequences. The introns-exons structure of *Li3CARS* was then compared with those of four previously reported TPSs from *Lavandula*.

A maximum likelihood phylogenetic tree was constructed based on deduced amino acids of mono- and sesquiterpene synthases using the default parameters of CLC Genomics Workbench 8.0.3 (https://www.qiagenbioinformatics.com/). TPSs were clustered into previously defined distinct TPS subfamilies (Bohlmann et al. 1998; Chen et al. 2011).

Homology-based molecular modeling

A homology model of Li3CARS protein was produced using the SWISS-MODEL automated mode server (Bordoli et al. 2009; Guex et al. 2009) after searching the best template. The crystal structure of *S. officinalis* bornyl pyrophosphate synthase (SoBPPS) (PDB code 1N1Z) containing the substrate analog diphosphate (POP) (Whittington et al. 2002) was detected as the top structural homologous template. The structural quality of the constructed model was verified using combined programs run in Structural Analysis and Verification Server (SAVeS) version 4 (http://nihserver.mbi.ucla.edu/SAVES/). The model underwent energy minimization using YASARA force field (Krieger et al. 2009), and energy-minimized 3D ligand for docking to the model was generated using the PRODRG server (Schüttelkopf and Van Aalten 2004). Docking studies with the model Li3CARS protein and GPP were conducted using autodock4 in molecular docking server (Bikadi and Hazai 2009). The position of substrate GPP from SoBPPS PDB 1N20 was used as docking positional template. Among the top five favorable positions of the ligand, the most energetically favorable position was selected. The docking result was visualized

and analyzed using PyMOL v1.1 (The PyMOL Molecular Graphics System, Schrödinger, LLC). Moreover, active site cavities were detected from the model using Swiss-pdbviewer (Guex et al. 2009), in which magnesium ions and binding residues at the active site pockets were docked into the model in positions corresponding to those observed in the SoBPPS template structure using both Swiss-pdbviewer and PyMOL v1.1 softwares.

Recombinant protein expression and purification

The ORF of *Li3CARS,* excluding the putative transit peptide sequence, was expressed in *E. coli* Rosetta™ (DE3)plysS cells (EMD Chemicals, Darmstadt, Germany). *E. coli* cells were grown in LB media supplemented with 30 mg L^{-1} kanamycin and 34 mg L^{-1} chloramphenicol at 37 °C to an OD_{600} of 0.5-0.7, followed by induction with 1 mM IPTG at 20 °C for overnight. After harvesting, the pelleted cells were resuspended in lysis buffer (50 mM NaH_2PO_4, 300 mM NaCl and 10 mM imidazol, pH 8.0) and were further disrupted by sonication. The crude protein was then purified using PerfectPro Ni-NTA Agarose chromatography (5Prime Gmbh, Germany), in which Ni-NTA agarose bound to His-tag recombinant proteins according to the manufacturer's instructional manual. Partially affinity-purified proteins were then quantified through a Bradford assay and resolved by SDS-PAGE.

Enzyme assays and product identification

The activity of partially purified recombinant Li3CARS was assayed with GPP, NPP and FPP as substrates. The assay reactions were prepared in a final volume of 500 µl, containing an enzyme reaction buffer (2 mM dithioerythreitol, 12.5 % (v/v) glycerol, 1 mM $MgCl_2$ and 1 mM $MnCl_2$), pH buffer, purified enzyme and substrates. The optimal assay pH was determined using MES (50 mM, pH 5.5-6.5) and MOPS (50 mM, pH 7.0-8.0) buffers, and the appropriate temperature was optimized between 27 °C and 40 °C. The assays were overlaid with 400 µl of pentane and were incubated for 10-90 min. The products were then extracted with pentane according to previous reports (Demissie et al. 2011; Demissie et al. 2012). Purified proteins from *E. coli* lysate cells harboring the empty pET41b(+) vector were also assayed with substrates as a negative control. Assay product identification and quantification were carried out using gas chromatography- mass spectrometry (GC-MS) following methods described in Demissie et al. (2012). Authentic standards of monoterpenes were also run on GC-MS under similar conditions to identify the products. The Michaelis-Menten enzymatic saturated curves were generated using GraphPad Prism 6 (GraphPad Software, Inc.). K_m and V_{max} values were estimated using the linear regression method of double-reciprocal plots (Lineweaver Burk) using the same software.

Induction of Li3CARS in L. x intermedia by MeJA

Approximately three months old *L. x intermedia* (cv Grosso) plants were used for MeJA induction experiments. The plants were sprayed with a 5 mM aqueous solution of MeJA (95% solution, Sigma-Aldrich) in water with 0.1 % Triton x-100 and water (mock treatment, control) supplemented with 0.1 % Triton x-100. The treated plants were then covered with Ziploc plastic bags for two hours and allowed to dry in open air for an hour before transferring them into a growth chamber. EO was extracted from fresh young leaves harvested at 0, 24, 48 and 72 h post-

treatments, and was used to determine EO compositions. Likewise, fresh young leaves at 0, 8, 24, 48 and 72 h post-treatments were harvested and flash-frozen in liquid nitrogen and kept at - 80 ºC for RNA extraction.

Relative expression

To quantify the constitutive (from flower and leaf tissues) and induced (leaves induced by MeJA) mRNA abundance for *Li3CARS*, a qPCR study was performed using the StepOne Plus Real-Time PCR system (Applied Bioscience). Total RNA was extracted from each collected sample using RNeasy Plant Mini Kit (Qiagen) according to the manufacturer's protocol. The RNA samples were then reverse transcribed using iScript cDNA synthesis Kit (Bio-Rad). Expression levels of the *Li3CARS* were normalized using *β-actin* and *18S rRNA* as internal reference genes. qPCR was performed with a final reaction volume of 10 µl, consisting of 5 µl SYBR premix, 0.6 µM of each primer and 150 ng of cDNA template. The amplification conditions were set with holding stage at 50 ºC for 2 min, and 95 ºC for 2 min, followed by 50 cycles at 95°C for 3 s and 60 °C for 30 s, as well as a final melting curve stage at 95 °C for 15 s and 60 °C for 1 min. For each qPCR run, the primer efficiency of every primer set used in this study was calculated using LinRegPCR (Ruijter et al. 2009). The generated data was analyzed using the Livak method (Livak and Schmittgen 2001), expressed as $2^{-\Delta\Delta CT}$ of *Li3CARS* gene. Three technical replicates were performed for each of the three independent biological replicates. The statistical analysis was made with Student's t-test using SigmaPlot v 12.5 (Systat Software, Germany). The primers used in this study are listed in Table 1.

EO extraction and GC-MS analysis

Approximately 0.5 g of MeJA-treated or mock (control) leaf samples were harvested and immediately placed in separate 50 mL test tubes containing 6 mL pentane and 160 µg thymol as an internal standard. This was followed by sonication on ice for 30 min. Pentane-containing EO from each sample was then run on a Varian CP 3800 GC coupled to a Saturn 2200 MS/MS. In brief, a 1 µl sample was injected with the following instrument setting. Column flow rate: 1 mL min^{-1}, injector temperature: 40 ºC for 10 s, and increased to 100 ºC (20 ºC min^{-1}) for the remaining of the run; column oven temperature: 40 ºC for 5 min, rise to 170 ºC at a rate of 6 ºC min^{-1}, hold for 4 min, then ramp to 230 ºC at a rate of 30 ºC min^{-1}, and hold for 5 min. The concentration of EO constituents in the MeJA-treated and control samples were calculated based on an internal standard (thymol) as previously described (Erland, 2015). Statistical analysis (Student's t-test) was performed using SigmaPlot v 12.5 (Systat Software, Germany).

Results

Sequence analysis of the Li3CARS

Using homology-based screening, we detected partial sequences of *Li3CARS* from ten ESTs from *L. x intermedia* flower glandular trichome-derived EST library (Demissie et al. 2012). The full length cDNA was then obtained from the corresponding cDNA library. The complete ORF of Li3CARS cDNA (Accession no.: KX024762) encoded a protein of 599 amino acids with a 45 amino acid plastid targeting sequence. The encoded protein was predicted to have a molecular mass of 69.6 kDa and a pI of 5.08. The deduced amino acid sequence was further characterized for

the conserved motifs against orthologous TPSs across the genus *Lavandula* and other angiosperms. As with other plant TPSs, the key motifs that are crucial for pernyl diphosphate ionization (RRx_8W), and for divalent metal ion binding (DDxxD and (N,D)D(L,I,V)x(S,T)x_3E) were well conserved in Li3CARS (Fig. 2). Additionally, the Li3CARS shared other conserved residues (LQLYEASFLL, presumed to involve in substrate binding) with plant TPSs. Further, Li3CARS exhibited high amino acid identity with *L. angustifolia* limonene synthase (75 %) and *S. officinalis* bornyl pyrophosphate synthase (SoBPPS) (65 %). Finely, Li3CARS was found to be less homologous to 3-carene synthases from *S. stenophylla* (~50 %) and *P. abies* (~29 %).

***Functional characterization of* Li3CARS**

Expression of the Li3CARS ORF in *E. coli* Rosetta™ (DE3) pLysS strain using pET41b(+) expression vector produced a soluble protein (64.9 kDa) that could be purified using Ni-NTA-agarose affinity chromatography. The partially purified protein was assayed for activity with GPP, NPP and FPP. The products of the reactions were analyzed by GC-MS. Different products were detected from assays of Li3CARS with GPP and NPP (Fig. 5). The activity of Li3CARS incubated with GPP (0.5 - 100 μM) extended from 10-90 min with optimum pH (7.0 - 7.5) (Fig. 6A) and temperature (30 ºC) conditions. Li3CARS converted GPP to 3-carene (~76%) and a few other minor products (24 %) (Table 2). The Michaelis-Menten enzymatic saturation curve was generated using GPP (Fig. 6B), and the corresponding double-reciprocal plot revealed the K_m and V_{max} values of 3.69 ± 1.17 μM and 128 ± 7.84 pkat/mg, respectively. The calculated values of k_{cat} and catalytic efficiency (k_{cat}/K_m) were 2.01 s^{-1} and 0.56 $\mu M^{-1}s^{-1}$, respectively.

Substrate preference of Li3CARS was examined by assaying the affinity-purified protein with NPP (the cisoid isomer of GPP) in similar conditions of GPP. The assay products analyzed by GC-MS revealed multiple products including limonene (33 %), terpinolene (29 %), α-thujene (20 %), α-phellanedrene (8.8 %) and 3-carene (8.5 %) (Table 2). To investigate the catalytic efficiency of Li3CARS with this particular substrate, we determined the kinetic properties using NPP over the concentration range of 1-150 μM. The enzyme activity showed typical Michaelis-Menten kinetics for all of these detected products (Fig. 6B & S2). The corresponding double reciprocal plots indicated that Li3CARS had apparent K_m values of 14 to 36 μM and V_{max} values ranging from 50 to 203 pkat/mg (Fig. 6D & S2, Table 3). The turnover (k_{cat}) of Li3CARS varied from 0.636 to 2.59 s^{-1} depending on the distribution of the products (Table 3). However, it had a comparable catalytic efficiency among the products with k_{cat}/K_m values ranging from 0.044 to 0.088 $\mu M^{-1}s^{-1}$. As a control, affinity-purified extracts from empty vector transformed *E. coli* Rosetta™ (DE3) pLysS, and boiled affinity-purified Li3CARS protein was assayed with GPP and NPP. The results showed that none of the aforementioned products from both substrates were detected from the control reactions.

Homology modeling of Li3CARS

To examine its 3D structure, we constructed a homology-based model of Li3CARS protein based on the crystal structure of SoBPPS (PDB identifier 1N1Z). Li3CARS (in particular the active site cavity) exhibited high structural

identity (66 %) to SoBPPS (Whittington et al. 2002). The integrity of the homology model was also verified with Procheck that resulted in a strong Ramachandran plot statistics of 92.2 % residues in most favored regions, 7.6 % allow and 0.2 % disallow residues among a total of 541 residues. As reported in SoBPPS 3D structure, the C-terminal domain of Li3CARS was predicted to have a potential active site cleft at different helices and loops (Fig. 7A). The two main helices were helix D and H, containing the aspartate-rich motif of DDxxD and (N,D)D(L,I,V)x(S,T)x_3E, respectively, at opposite walls of the active site (Fig. 2 & 7). As the important residues within the SoBPPS active site are well known (Whittington et al. 2002), the active site cavity of Li3CARS was computed (Fig. 7B). Several residues residing on the surface of the active site were predicted, some of which could play paramount roles in substrate binding and selectivity. There were also exceptions showing differences at Li3CARS residues N428, I454 and S455 compared to the SoBPPS template (Fig. 7C). In addition to the main active site helices (D and H), two regulatory loops (H-α1 and J-K) were predicted on the Li3CARS model structure with few Li3CARS-specific residues, such as V574, D575, I584 and I585, at H-α1 (A507) and at J-K loops (Fig. 2). Moreover, in an attempt to find the possible binding sites of substrates on Li3CARS protein, docking study with GPP and the model Li3CARS protein was conducted. The results revealed that most of the aforementioned active site residues play active roles in the interaction of GPP and Li3CARS protein (Fig 7D & E). Among the detected active site amino acid residues, D353, D357, R497, D497, T501 and E505 residing on helix D and H were predicted to play a role in the binding of GPP (particularly the phosphate group), and in Mg^{2+} ion coordination.

Genomic DNA organization and phylogenetic analysis

Genomic sequence of the *Li3CARS* was amplified from genomic DNA extracted from *L. x intermedia* leaves and characterized to understand its evolutionary relationship with TPSs from *Lavandula*. The complete genomic sequence of *Li3CARS* (Accession no.: KX024761) was 2782 bp long and contained a typical intron-exon structure of *Lavandula* and other angiosperms *TPS*-a and *TPS-b* subfamily genes, bearing 7 exons interrupted with 6 introns (Fig. 3A). Every exon and intron junction of *Li3CARS* showed an identical pattern of ~NNN▾GT at 3′ and AG▾NNN~ at 5′, in which 'NNN' represents sequences of exons (Fig. S1). A comparison with previously reported genomic DNA of *Lavandula* TPSs showed that *Li3CARS* was highly homologous to these TPSs in terms of exon size (Fig. 3A). The length of exon4 remained conserved in all of the five TPSs, whereas *Li3CARS* bore unique lengths at exon3 and exon7. Most of the exons, such as exon1, exon4, exon6 and exon7 contained the common TPS conserved motifs at the expected positions. Intron sizes were the most variable genomic structures among the five *Lavandula* TPSs (Fig. 3B). The shortest and longest introns in the five *Lavandula* TPSs were intron-4 (58 bp) in *LiCINS* and intron-1 (926 bp) in *LaLINS*, respectively. Those introns were replaced by a small size intron-2 (70 bp) and a large size intron-3 (430 bp) in *Li3CARS*.

Based on their amino acid sequences, we constructed a neighbor joining phylogenetic tree for Li3CARS along with some TPSs subfamilies of angiosperms and gymnosperms (Fig. 4). The tree showed that *Li3CARS* was clustered into the TPS-b subfamily. The TPS-b subfamily members were further divided into three subclades (I, II & III). The two angiosperm 3-carene synthases - *S. stenophylla* 3-carene synthase and *L. x intermedia Li3CARS* - were grouped

separately under subclade II and III, respectively. More specifically, *Li3CARS* had a very close evolutionary relationship to that of *L. angustifolia* limonene synthase under the same subclade III. Most angiosperms sesqui-TPSs and gymnosperm TPSs, including *P. abies* 3-carene synthase, were categorized into TPS-a and TPS-d subfamilies, respectively.

Relative expression of the Li3CARS

Because of the low EST copy numbers of the candidates from flower glandular trichomes, we predicted that *Li3CARS* is either differentially expressed or induced by other factors. To test this hypothesis, we performed a spatial qPCR study in *L. x intermedia* leaf and flower tissues. The relative expression results showed that *Li3CARS* transcripts were 16 fold more abundant in leaves compared to flowers. The expression pattern of *Li3CARS* was also examined in response to MeJA application. MeJA induced *Li3CARS* transcript levels in leaves (Fig. 8) significantly (2.5-3.8 fold) ($P \leq 0.05$) as early as 8 hours post-treatment. Not surprisingly, this up-regulation declined after 24 h post-treatment and reached to a low transcript level at 72 h post-treatment, which was a comparable expression pattern to the corresponding control leaf tissues.

Monoterpene accumulation in L. x intermedia

Monoterpene content was quantified in the flowers and leaves of *L. x intermedia* plants in order to determine the in *planta* contribution of *Li3CARS* to EO metabolism. Despite variations in quantity, most of the products obtained from the *Li3CARS in vitro* assay were detected in leaf tissue (Fig. S3) where the gene is strongly expressed. Further, MeJA had a strong impact ($P \leq 0.05$) on the contents of 3-carene and limonene at 24 and 48 h post-treatment (Fig. 9). 3-Carene content reached a maximum in MeJA treated tissues with 200 ng mg^{-1} higher than its control at 48 h post treatment. Limonene concentration also increased by nearly 95 ng mg^{-1} of fresh leaf tissue over its control at 24 h post-treatment. The tissue levels of both 3-carene and limonene remained constant after 48 h post-treatment. The accumulation of α-thujene - Li3CARS *in vitro* assay product from NPP - were less affected with 5 mM MeJA in all tested exposure time courses (Fig. 9).

Discussion

Li3CARS sequences has typical mTPS conserved motifs

Availability of public sequence databases facilitates the isolation and functional study of genes using homology-based cloning. In this study, we isolated *Li3CARS* from *L. x intermedia* glandular trichome (Demissie et al. 2012) that encoded 599 amino acids consisting of major conserved motifs present in typical plant TPSs (Fig. 2). Most of the conserved motifs have been well characterized in TPSs, among which the first motif located at the very beginning of N-terminus of the protein is RR(x8)W required in mTPSs for cyclization (Williams et al. 1998), or protein stabilization (Hyatt et al. 2007). The second and third motifs presented at C-terminus were DDxxD and (N,D)D(L,I,V)x(S,T)xxxE, in which both are responsible for substrate binding and coordination of divalent metal ion cofactors (Degenhardt et al. 2009). Another conserved motif, LQLYEASFLL, in Li3CARS is thought to be a

part of the active site components in SoBPPS (Wise et al. 1998). Alterations of the common residues are often observed in these motifs from sesqui-TPSs. For example, cadinol and germacrene D synthases from *L. angustifolia* contain deletion and/or substitution of one arginine (R) at RR(x8)W motif, whereas one aspartate (D) is substituted by glutamate (E) at DDxxD of germacrene D synthases (Jullien et al. 2014).

Li3CARS has high affinity to GPP

The genes and encoding enzymes for some of the major *Lavandula* monoterpenes biosynthesis have been identified and functionally characterized *in vitro* from economically important species, including *L. angustifolia* and *L. x intermedia* (Landmann et al. 2007; Demissie et al. 2011; Demissie et al. 2012). The clone *Li3CARS* was found to be an mTPS that catalyzes the conversion of GPP, the universal precursor of the monoterpenes, to 3-carene, and a few other minor products. Generation of major and minor monoterpenes by Li3CARS activity from GPP was not a surprise, as multi-product mTPS from both angiosperms and gymnosperms are well known (Wise et al. 1998; Fäldt et al. 2003; Demissie et al. 2012). The distribution of 3-carene (76 %) produced *in vitro* by Li3CARS is in close range to 3-carene generated by 3-carene synthases from *S. stenophylla* (Hoelscher et al. 2003) and from *P. abies* (Fäldt et al. 2003), accounting for 73 % and 78 %, respectively. However, there are species-specific minor products with distinct distributions, such as myrcene (6 %), 4-carene (4 %) and β-phellandrene (1 %) from *S. stenophylla* (Hoelscher et al. 2003); myrcene (3%), terpinolene (11%), limonene (0.4 %) and β-phellandrene (0.7%) from *P. abies* (Fäldt et al. 2003); and β-pinene (5.8 %), limonene (9.3 %) and 2-carene (8.7 %) from *L. x intermedia* (Table 2). Variations among minor products with discrete distribution would be expected, as the Li3CARS enzyme is not identical to others, in that it shares only 50 % and 28 % amino acids homology to 3-carene synthase from *S. stenophylla* and *P. abies*, respectively.

Although the kinetic properties of 3-carene synthase have not yet been studied in *Lamiaceae*, such investigations have been conducted in coniferous plants (Savage and Croteau, 1993; Hall et al. 2011). The optimum assay conditions for Li3CARS activity with GPP were found to be similar to most of lavender mTPSs (Demissie et al. 2011; Demissie et al. 2012) and 3-carene synthases of *S. stenophylla* and *P. abies* (Savage and Croteau, 1993; Hoelscher et al. 2003). High catalytic efficiency of Li3CARS was apparent with K_m= 3.692 ± 1.17 µM and k_{cat} = 2.07 s^{-1}, which appear to be in close range of the K_m (1.47 - 8.09 µM) and k_{cat} (0.06-2.25 s^{-1}) values of coniferous 3-carene synthases (Savage and Croteau, 1993;Hall et al. 2011). However, Li3CARS displayed a lower K_m (3.692 ± 1.17 µM) value than that of the most common mTPSs from *Lavandula,* including β-phellandrene synthase (6.55 ± 1.01 µM), 1,8-cineole synthase (5.75 ± 0.91 µM), linalool synthase (47.7 ± 4.6 µM) and limonene synthase (47.4 ± 3.8 µM) (Landmann et al. 2007; Demissie et al. 2011; Demissie et al. 2012). This low K_m value indicates that Li3CARS has a strong affinity to GPP compared to the rest of previously identified mTPSs from *Lavandula*.

Most *Lavandula* mTPSs accept both GPP and NPP as substrates, producing comparable amounts of the same end products (Demissie et al. 2011; Demissie et al. 2012). However, the recombinant Li3CARS converted NPP to a different set of compounds than those it derived from GPP. While GPP was converted mainly to 3-carene, NPP was

transformed into limonene (33 %), terpinolene (29 %) and α-thujene (20 %) as main products, and minor amounts of a few other monoterpenes including 3-carene (8.5 %) (Table 2). The catalytic efficiency (k_{cat}/K_m) of Li3CARS to produce 3-carene was nearly 13-fold lower when NPP, rather than GPP, was used as a substrate (Table 3). However, Li3CARS displayed a higher catalytic efficiency for producing limonene and terpinolene from NPP than GPP. Taken together, these results indicate that substrate availability may play a key role in the production of certain monoterpenes in plants. It must be noted that the gene and encoding enzyme for NPP biosynthesis have not yet been identified in *Lavandula*. Therefore what is observed in *in vitro* assays may not occur *in planta*. This argument is supported by the fact that products derived from NPP by recombinant Li3CARS may also be obtained from GPP by various mTPSs in lavenders. For example, *L. angustifolia* limonene synthase (LaLIMS) converts GPP to limonene (Landmann et al. 2007). EO extracted from *L. x intermedia* leaves is also abundantly composed of the monoterpenes that are mainly the products of recombinant Li3CARS from GPP (Fig. 5B). Despite the fact that recombinant Li3CARS catalyzed both GPP and NPP, the native Li3CARS enzyme more likely uses GPP as a substrate in lavenders plant cells to produce the major product of 3-carene and other minor monoterpenes.

Li3CARS 3D protein model construction

Knowledge of the 3D structures of a given protein is indispensable for obtaining insight into the molecular basis of protein function. In the absence of experimental data, protein models can be built from known 3D structures of homologous protein templates using modeling software such as SWISS-MODEL (Bordoli et al. 2009; Guex et al. 2009). In this study, a homology model was built for Li3CARS (Fig. 7) using a 3D structure of SoBPPS (Whittington et al. 2002) as a template. The alignment of Li3CARS and SoBPPS revealed strong homology of the active site, except for a few residues (N428, I454 and S455). An active site with broad ranges of residues seem to be more elastic to accommodate the series of carbocation rearrangements, and produce distinct multi-products, as demonstrated from SoBPPS and *Mentha* limonene synthase (Whittington et al. 2002; Hyatt et al. 2007). As shown in Fig. 7, both divalent metal ions binding helices (D and H), and the loops (H-α1 and J-K), which play significant roles in GPP binding and catalytic activity of Li3CARS, are in line with features obtained from the SoBPPS template (Whittington et al. 2002), except a few residues at H-α1 (A507) and at J-K loop, such as V574, D575, I584 and I585. Like most TPSs, the Li3CARS structure reveals the conservation of the two aspartate-rich motifs that coordinate to the metal ions (Rynkiewicz et al. 2001; Whittington et al. 2002; Hyatt et al. 2007). The homology-based protein structure with GPP docking confirmation will ultimately provide input for further exploring the molecular mechanisms of 3-carene synthase and/or other TPSs in *Lavandula*. For example, potential amino acid residues responsible for catalytic activity with GPP and other intermediates may further be identified and studied through mutational analysis.

Evolutionary inference from Lavandula TPS genes

As evidenced by the protein analysis data, *Li3CARS* is highly homologous to the *L. angustifolia* limonene synthase (*LaLIMS*), and is clustered with this gene under angiosperm mTPSs (TPS-b) subfamily (Bohlmann et al. 1998). However, *Li3CARS* had low homology to limonene synthases and 3-carene synthases from other species

(Fig. 4). This indicates that *LaLIMS* and *L. x intermedia Li3CARS* originated from the same ancestor or one has evolved from the other through gene duplication, which could fuel divergent functional evolution leading to sub-functionalization and / or neofunctionalization of mTPSs. It is not surprising that *Li3CARS* is more homologous to other *Lavandula* TPSs rather than to 3-carene synthases from other species, as this phenomenon (that TPSs genes with different functions are more homologous to each other within a given species rather that TPSs with the same function in a different species) has been observed in several cases before. For example, in Sitka spruce, (+)-3-carene synthase family genes share 89-92 % nucleotides identity with (-)-sabinene synthase, but a single amino acid at a specific position determined the plasticity and evolution of both enzymes functions (Roach et al. 2014).

The genomic structure of *Li3CARS* contained typical features of the Class III TPSs, bearing seven exons and six introns (Chen et al. 2011). It also exhibited similar patterns of exon-intron structures to TPSs in most of angiosperms.

Li3CARS is differentially expressed

To gain insight into the potential biological role of 3-carene in lavenders, we examined tissue specific transcriptional expression of *Li3CARS* by qPCR. The results indicated that *Li3CARS* is more strongly expressed in leaves than in flowers of *L. x intermedia* plants. The high transcript levels for this gene in leaves correlated well with the accumulation of 3-carene in leaf tissue, indicating that production of 3-carene is regulated (at least in part) through the transcriptional regulation of *Li3CARS*. In this context, a high concentration of 3-carene has been reported in peltate glandular trichomes of *S. stenophylla* (Hoelscher et al. 2003), and shoots and foliage of *P. abies* (Fäldt et al. 2003), where the corresponding *3-carene synthase* genes are highly expressed.

The transcriptional expression of *Li3CARS* was induced by MeJA. Transcript levels for the gene were temporarily elevated upon MeJA application to a maximum at 24 h post-treatment, which positively correlated to the leaf 3-carene concentrations. This outcome is not surprising as MeJA is a known inducer of TPS genes expression in plants. For example, MeJA increased the expression of genes involved in volatile compound formation 12 h and 24 h post-treatment (Shi et al. 2015). Similarly, several mTPSs and sesquiTPSs were induced with MeJA treatment in *P. abies,* lima bean, tomato and *A. sinensis* (Martin et al. 2002; Van Schie et al. 2007; Menzel et al. 2014; Xu et al. 2016).

The up-regulation of *Li3CARS* transcripts by MeJA treatment points to potential defensive role for this gene in *Lavandula*, in particular in young leaves (where 3-carene is mainly produced) that are more prone to insect and pathogen attack. This postulate is supported by several lines of evidence. For example, previous findings demonstrated that several monoterpenes, in particular 3-carene, are toxic to insects and pathogens (Fäldt et al. 2003; Fujimoto et al. 2011; War et al. 2011). In this context, EOs of various plants (including lavenders) have been used in controlling important insects and microbes *in vitro* (Moon et al. 2006; De Rapper et al. 2013; Erland et al. 2015). This is also supported by reports that production of certain defensive monoterpenes, including 3-carene, myrcene, α-

pinene, and limonene, in various plants, is induced in response to MeJA, mechanical wounding, pathogen infection and herbivore attack (Martin et al. 2002; Robert et al. 2010). Further, the expression of several mTPS genes, including (+)-3-carene synthase and linalool synthase, is regulated by MeJA, and by pathogens and insects in tomato, rice, lima beans, sitka spruce and pine trees (Van Schie et al. 2007; Moreira et al. 2009; Robert et al. 2010; Menzel et al. 2014; Taniguchi et al. 2014). Despite the above arguments, it should be noted that direct evidence for a defensive role for 3-carene in *Lavandula* is missing at this point. However, in the light of our result this area is worth exploring.

Conclusion

We have isolated and functionally characterized a 3-carene synthase (Li3CARS) cDNA from *L. x intermedia*. The homology-based 3D structure of Li3CARS was deduced from which the active site residues were identified. The protein exhibits strong homology to Class III TPSs and is grouped under the *TPS-b* subfamily. *Li3CARS* is constitutively expressed in both leaf and floral tissues, although expression is much stronger in leaves. Both *Li3CARS* transcript and 3-carene levels were significantly up-regulated by methyl jasmonate, and point to a potential induced defensive role for 3-carene in lavenders.

Legends

Figures

Fig. 1. Schematic representation of the biosynthesis of monoterpenes catalyzed by recombinant Li3CARS from geranyl pyrophosphate (GPP) and neryl pyrophosphate (NPP). While Li3CARS produced 3-carene (bold) as a major product from GPP, i.e. the enzyme derives almost equal amounts of the shown monoterpenes from NPP.

Fig. 2. Sequence alignment of Li3CARS (KX024762) with SoBPPS (AAC26017.1), LaLIMS (ABB73044.1), Ss3CARS (AF527416.1) and Pa3CARS (AAO73863.1). The predicted transit peptide is underlined, and the main TPS conserved motifs are overlaid with bars. The major helices and loops, predicted based on the homology–based (to SoBPPS) 3D structures of Li3CARS crystal structure, are marked underneath the respective sequences. Helices are labeled D (G336-D357), H (D484-L506), α1 (A514-E521), J (Y556-V572) and K (Q588-M594), and loops are labeled H-α1 (K507-K513) and J-K (Y573-I587).

Fig. 3. Schematic presentation of *Li3CARS* genomic DNA organization from *L. x intermedia* (cv Grosso) in comparison with previously reported *Lavandula* TPSs genomic DNAs (**A**). Comparison of intron lengths among *Lavandula* TPSs (**B**). Exons with rectangular boxes are connected with lines of introns (1 - 6). Every exon length is measured by amino acids (shown in the box). The approximate locations of the main conserved motifs are indicated by arrows at Exon1, Exon4, Exon6 and Exon7. The three TPSs, such as LaLIMS- limonene synthase, LaLINS-

linalool synthase and LaBERS- trans-α-bergamotene synthase from *L. angustifolia*, are adapted from Landmann et al. (2007), while *L. x intermedia* 1,8-cineole synthase (LiCINS) is adapted from Demissie et al. (2012).

Fig. 4. **A**) The maximum likelihood phylogenetic analysis of some plant monoterpenes and sesquiterpne synthases using neighbour joining method. **B**) *Lavandula* TPSs that are identified and functionally characterized so far, except α-pinene synthase from *Lavandula viridis* (Lv_a-pinene_S), are further compared separately. Numbers at each node represents bootstrap percentage. The deduced amino acid sequences are used for phylogenetic comparison. The related accession numbers and source species for a particular gene / protein are listed in Table S1.

Fig. 5. Gas chromatography of monoterpenes generated by recombinant Li3CARS from NPP and GPP substrates. Assay products of Li3CARS from NPP (**A**) and GPP (**B**), as well as authentic standards of 3-carene and limonene (**C**). Detected monoterpenes from both substrates are α-thujene, β-pinene, α-phellandrene, 3-carene, limonene, 2-carene and terpinolene. Camphor (200 ng/ml) was used as internal standard.

Fig. 6. Kinetic assay of affinity-purified recombinant Li3CARS with GPP and NPP as substrates. Li3CARS activity across different pH levels (**A**). Velocity of Li3CARS activity at increasing concentrations of GPP (0.5 - 100 µM) (**B**) and NPP (1 -150 µM) (**C**) to produce 3-carene. Double-reciprocal plots for determining the K_m and V_{max} of Li3CARS from GPP (**D**) and NPP (**E**). Michaelis-Menten kinetic parameters from GPP and NPP are; K_m = 3.69 ± 1.17 and 14.3 ± 2.56 µM, V_{max} = 128 ± 7.84 and 49.9 ± 2.37 pkat/mg, k_{cat} (V_{max}/[E]) = 2.07 and 0.636 s^{-1} as well as k_{cat}/K_m= 0.561 and 0.044 $\mu M^{-1}s^{-1}$, respectively.

Fig. 7. The 3D structural model of Li3CARS protein, built based on the crystal structure of SoBPPS (PDB identifier no of 1NZ1). **A**) A monomer of Li3CARS showing the potential active site at C-terminal domain, the predicted helical segments and aspartate-rich residues (blue). **B**) The computed surface structure of Li3CARS displaying the main active site (red mesh) with binding residues (blue sticks) and predicted divalent metal ion (green sphere). **C**) The Li3CARS active site cavity with residues bound to the surface of the cavity. The two aspartate-rich motifs (**D**Dxx**D** and (N,**D**)D(**L**,I,V)x(S,**T**)x_3**E**)) are green, in which a Mg^{2+} ion (red sphere) binds to the motif. Other residues potentially involved in substrate binding and selectivity are highlighted in orange, of which residues of N428, I454 and S455 are found to be specific to Li3CARS. **D**) Docked confirmation of GPP with respect to the active site residues in model Li3CARS protein, and **E**) the major residues residing in the active site involved in the binding and catalytic activity of GPP. Metal coordination and direct interactions of active site residues and the phosphate groups of GPP are indicated dashed blue lines. GPP ligand is shown in green (the C_{10} carbon) and in pink and orange (the phosphate group).

Fig. 8. Quantitative real-time PCR analysis for temporal expression of *Li3CARS* from *L. x intermedia*. Induced expression patterns of *Li3CARS* from young plant foliage were assessed using MeJA (5 mM) for three time courses compared with mock treated samples. Mock samples (controls) were treated with water supplemented with 0.1%

Triton x-100. The control was assigned with the arbitrary value of 1.0. *Li3CARS* transcript levels were normalized to *β-actin* and *18S rRNA* genes. Results represent mean values of biological replicates ± standard errors (*n=3*), $**P \leq 0.01$.

Fig. 9. Accumulation of monoterpenes (ng mg^{-1} fresh weight) (mean ± standard errors) in young *L. x intermedia* plants in response to 5 mM MeJA treatment. **A**) 3-Carene, **B**) α-thujene and **C**) limonene. Mock samples were treated with water supplemented with 0.1% Triton x-100. Asterisk (*) indicates significant differences ($* = P< 0.05$) between MeJA treated and mock (control) in Student's t-test. Bars show standard errors (*n=4*).

Tables

Table 1. List of all primer sets used in this study.

Table 2. Distribution of products from *in vitro* enzymatic assay of recombinant Li3CARS using GPP and NPP as substrates. Means in peak areas and standard errors are calculated from four independent experiments. The major product from GPP is shown in bold.

Table 3. Comparison of the kinetic properties of recombinant Li3CARS using GPP and NPP as substrates.

Supplementary data

Fig. S1. Genomic sequence obtained from *L. x intermedia* (cv Grosso) with exon and intron junctions that are highlighted with color (yellow). Sequences with red selection are introns, as well as start and stop codons are bold and underlined.

Fig. S2. Kinetic analysis of Li3CARS using NPP with respect to different products. The Michaelis-Menten saturated curve of Li3CARS by measuring (**A**) α-thujene, (**B**) limonene and (**C**) terpinolene, and the double-reciprocal plot of Li3CARS for (D) α-thujene, (E) limonene and (F) terpinolene.

Fig S3. A full leaf monoterpene profile of *L. x intermedia* (cv. Grosso). **A**) A gas chromatogram of monoterpenes and **B**) their distribution in leaf essential oil. Means in peak areas and standard errors are calculated from seven independent samples. Unidentified monoterpenes are labeled from 1-7.

Table S1. Diverse plant TPSs with the corresponding GenBank/ UniProt accession numbers that are incorporated in the phylogenetic analysis of *Li3CARS* gene.

Acknowledgement

This work was supported through grants and/or in-kind contributions to SSM by UBC, Genome British Columbia, Natural Sciences and Engineering Research Council of Canada, Agriculture and Agri-Food Canada and the BC Ministry of Agriculture (through programs delivered by the Investment Agriculture Foundation of BC).

References

Boeckelmann A (2008) Monoterpene production and regulation in Lavenders (*Lavandula angustifolia* and *Lavandula x intermedia*). MSc Thesis, University of british Columbia, pp:70-71.

Bohlmann J, Meyer-Gauen G, Croteau R (1998) Plant terpenoid synthases: molecular biology and phylogenetic analysis. Proc Natl Acad Sci U S A 95:4126–4133. doi: 10.1073/pnas.95.8.4126

Boone CK, Aukema BH, Bohlmann J, Carroll AL, Raffa KF (2011) Efficacy of tree defense physiology varies with bark beetle population density: a basis for positive feedback in eruptive species. Can J For Res 41:1174–1188. doi: 10.1139/x11-041

Bordoli L, Kiefer F, Arnold K, Benkert P, Battey J, Schwede T (2009) Protein structure homology modeling using SWISS-MODEL workspace. Nat Protoc 4:1–13. doi: 10.1038/nprot.2008.197

Burke CC, Wildung MR, Croteau R (1999) Geranyl diphosphate synthase: cloning, expression, and characterization of this prenyltransferase as a heterodimer. Proc Natl Acad Sci U S A 96:13062–13067. doi: 10.1073/pnas.96.23.13062

Byun-McKay A, Godard K-A, Toudefallah M, Martin DM, Alfaro R, King J, Bohlmann J, Plant AL (2012) Wound-induced terpene synthase gene expression in Sitka spruce that exhibit resistance or susceptibility to attack by the white pine weevil. New Phytol 3:3043–3052. doi: 10.1104/pp.105.071803

Chen F, Tholl D, Bohlmann J, Pichersky E (2011) The family of terpene synthases in plants: A mid-size family of genes for specialized metabolism that is highly diversified throughout the kingdom. Plant J 66:212–229. doi: 10.1111/j.1365-313X.2011.04520.x

Danet JL, Sémétey O, Gaudin J, Verdin E, Chaisse E, Foissac X (2010) Lavender decline is caused by several genetic variants of the stolbur phytoplasma in south eastern France. COST-2010, 9.

Degenhardt J, Köllner TG, Gershenzon J (2009) Monoterpene and sesquiterpene synthases and the origin of terpene skeletal diversity in plants. Phytochemistry 70:1621–1637. doi: 10.1016/j.phytochem.2009.07.030

Demissie ZA, Cella MA, Sarker LS, Thompson TJ, Rheault MR, Mahmoud SS (2012) Cloning, functional characterization and genomic organization of 1,8-cineole synthases from Lavandula. Plant Mol Biol 79:393–411. doi: 10.1007/s11103-012-9920-3

Demissie ZA, Erland LAE, Rheault MR, Mahmoud SS (2013) The biosynthetic origin of irregular monoterpenes in Lavandula: isolation and biochemical characterization of a novel cis-prenyl diphosphate synthase gene, lavandulyl diphosphate synthase. J Biol Chem 288:6333–41. doi: 10.1074/jbc.M112.431171

Demissie ZA, Sarker LS, Mahmoud SS (2011) Cloning and functional characterization of β-phellandrene synthase from Lavandula angustifolia. Planta 233:685–96. doi: 10.1007/s00425-010-1332-5

1 Dudareva N, Klempien A, Muhlemann JK, Kaplan I (2013) Biosynthesis, function and metabolic engineering of
2 plant volatile organic compounds. New Phytol 198:16–32. doi: 10.1111/nph.12145

3 Erland LAE (2015) Enhancement of specialized metabolism, regeneration efficiency and biological activity in
4 lavandin (*Lavandula* x *intermedia* cv 'Grosso'). MSc Thesis, University of british Columbia, pp:40-41

5 Erland LAE, Rheault MR, Mahmoud SS (2015) Insecticidal and oviposition deterrent effects of essential oils and
6 their constituents against the invasive pest Drosophila suzukii (Matsumura) (Diptera: Drosophilidae). Crop
7 Prot 78:20–26. doi: 10.1016/j.cropro.2015.08.013

8 Fäldt J, Martin D, Miller B, Rawat S, Bohlmann J (2003) Traumatic resin defense in Norway spruce (Picea abies):
9 Methyljasmonate-induced terpene synthase gene expression, and cDNA cloningand functional
10 characterization of (+)-3-carene synthase. Plant Mol Biol 51:119–133.

11 Fontana A, Held M, Fantaye CA, Turlings TC, Degenhardt J, Gershenzon J (2011) Attractiveness of Constitutive
12 and Herbivore-Induced Sesquiterpene Blends of Maize to the Parasitic Wasp Cotesia marginiventris
13 (Cresson). J Chem Ecol 37:582–591. doi: 10.1007/s10886-011-9967-7

14 Frost CJ, Appel HM, Carlson JE, De Moraes CM, Mescher MC, Schulz JC (2007) Within-plant signalling via
15 volatiles overcomes vascular constraints on systemic signalling and primes responses against herbivores. Ecol
16 Lett 10:490–498. doi: 10.1111/j.1461-0248.2007.01043.x

17 Fujimoto T, Tomitaka Y, Abe H, Tsuda S, Futai K, Mizukubo T (2011) Expression profile of jasmonic acid-induced
18 genes and the induced resistance against the root-knot nematode (Meloidogyne incognita) in tomato plants
19 (Solanum lycopersicum) after foliar treatment with methyl jasmonate. J Plant Physiol 168:1084–1097. doi:
20 10.1016/j.jplph.2010.12.002

21 Guex N, Peitsch MC, Schwede T (2009) Automated comparative protein structure modeling with SWISS-MODEL
22 and Swiss-PdbViewer: A historical perspective. Electrophoresis 30:162–173. doi: 10.1002/elps.200900140

23 Hall DE, Robert JA, Keeling CI, Domanski D, Quesada AI, Jancsik S, Kuzyk MA, Hamberger B, Borchers CH,
24 Bohlmann J (2011) An integrated genomic, proteomic and biochemical analysis of (+)-3-carene biosynthesis
25 in Sitka spruce (Picea sitchensis) genotypes that are resistant or susceptible to white pine weevil. Plant J
26 65:936–948. doi: 10.1111/j.1365-313X.2010.04478.x

27 Hasegawa M, Mitsuhara I, Seo S, Imai T, Koga J, Okada K, Yamane H, Ohashi Y (2010) Phytoalexin accumulation
28 in the interaction between rice and the blast fungus. Mol Plant Microbe Interact 23:1000–1011. doi:
29 10.1094/MPMI-23-8-1000

30 Heiling S, Schuman MC, Schoettner M, Mukerjee P, Berger B, Schneider B, Jassbi AR, Baldwin IT (2010)
31 Jasmonate and ppHsystemin regulate key Malonylation steps in the biosynthesis of 17-
32 Hydroxygeranyllinalool Diterpene Glycosides, an abundant and effective direct defense against herbivores in
33 Nicotiana attenuata. Plant Cell 22:273–292. doi: 10.1105/tpc.109.071449

34 Hoelscher DJ, Williams DC, Wildung MR, Croteau R (2003) A cDNA clone for 3-carene synthase from Salvia
35 stenophylla. Phytochemistry 62:1081–1086. doi: 10.1016/S0031-9422(02)00674-X

Huang M, Abel C, Sohrabi R, Petri J, Haupt I, Cosimano J, Gershenzon J, Tholl D (2010) Variation of herbivore-induced volatile terpenes among Arabidopsis ecotypes depends on allelic differences and subcellular targeting of two terpene synthases, TPS02 and TPS03. Plant Physiol 153:1293–310. doi: 10.1104/pp.110.154864

Hyatt DC, Youn B, Zhao Y, Santhamma B, Coates RM, Croteau RB, Kang C (2007) Structure of limonene synthase, a simple model for terpenoid cyclase catalysis. Proc Natl Acad Sci U S A 104:5360–5365. doi: 10.1073/pnas.0700915104

Jullien F, Moja S, Bony A, Legrand S, Petit C, Benabdelkader T, Poirot K, Fiorucci S, Guitton Y, Nicole F, Baudino S, Magnard JL (2014) Isolation and functional characterization of a τ-cadinol synthase, a new sesquiterpene synthase from Lavandula angustifolia. Plant Mol Biol 84:227–241. doi: 10.1007/s11103-013-0131-3

Landmann C, Fink B, Festner M, Dregus M, Engel KH, Schwab W (2007) Cloning and functional characterization of three terpene synthases from lavender (Lavandula angustifolia). Arch Biochem Biophys 465:417–429. doi: 10.1016/j.abb.2007.06.011

Lane A, Boecklemann A, Woronuk GN, Lukman S, Mahmoud SS (2010) A genomics resource for investigating regulation of essential oil production in Lavandula angustifolia. Planta 231:835–45. doi: 10.1007/s00425-009-1090-4

Livak KJ, Schmittgen TD (2001) Analysis of relative gene expression data using real-time quantitative PCR and the 2^(-ΔΔCT) method. Methods 25:402–408. doi: 10.1006/meth.2001.1262

Martin D, Tholl D, Gershenzon J (2002) Methyl Jasmonate Induces Traumatic Resin Ducts , Terpenoid Resin Biosynthesis , and Terpenoid Accumulation in Developing Xylem of Norway Spruce Stems 1. Society 129:1003–1018. doi: 10.1104/pp.011001.McGarvey

Menzel TR, Weldegergis BT, David A, Boland W, Gols R, Van Loon JJA, Dicke M (2014) Synergism in the effect of prior jasmonic acid application on herbivore-induced volatile emission by Lima bean plants: Transcription of a monoterpene synthase gene and volatile emission. J Exp Bot 65:4821–4831. doi: 10.1093/jxb/eru242

Miller B, Madilao LL, Ralph S, Bohlmann J (2005) Insect-induced conifer defense. White pine weevil and methyl jasmonate induce traumatic resinosis, de novo formed volatile emissions, and accumulation of terpenoid synthase and putative octadecanoid pathway transcripts in Sitka spruce. Plant Physiol 137:369–382. doi: 10.1104/pp.104.050187

Moon T, Wilkinson JM, Cavanagh HMA (2006) Antibacterial activity of essential oils, hydrosols and plant extracts from Australian grown Lavandula spp. Int J Aromather 16:9–14. doi: 10.1016/j.ijat.2006.01.007

Moreira X, Sampedro L, Zas R (2009) Defensive responses of Pinus pinaster seedlings to exogenous application of methyl jasmonate: Concentration effect and systemic response. Environ Exp Bot 67:94–100. doi: 10.1016/j.envexpbot.2009.05.015

Navia-Giné WG, Gomez SK, Yuan J, Chen F, Korth KL (2009) Insect-induced gene expression at the core of volatile terpene release in Medicago truncatula. Plant Signal Behav 4:639–41. doi: 10.1016/j.plaphy.2009.01.008

Ott DS, Yanchuk AD, Huber DPW, Wallin KF (2011) Genetic Variation of Lodgepole Pine, Pinus contorta var. latifolia, Chemical and Physical Defenses that Affect Mountain Pine Beetle, Dendroctonus ponderosae, Attack and Tree Mortality. J Chem Ecol 37:1002–1012. doi: 10.1007/s10886-011-0003-8

Williams DC, Mcgarvey DJ,Katahira EJ, Croteau R (1998) Truncation of Limonene Synthase Preprotein Provides a Fully Active " Pseudomature " Form of This Monoterpene Cyclase and Reveals the Function of the amino-terminal arginine pair. Biochemistry 37:12213–12220.

De Rapper S, Kamatou G, Viljoen A, Van Vuuren S (2013) The in vitro antimicrobial activity of Lavandula angustifolia essential oil in combination with other aroma-therapeutic oils. Evidence-based Complement Altern Med. doi: 10.1155/2013/852049

Rivera SB, Swedlund BD, King GJ, Bell RN, Hussey CE, Shattuck-Eidens DM, Wrobel WM, Peiser GD, Poulter CD (2001) Chrysanthemyl diphosphate synthase: isolation of the gene and characterization of the recombinant non-head-to-tail monoterpene synthase from Chrysanthemum cinerariaefolium. Proc Natl Acad Sci USA 98:4373–4378. doi: 10.1073/pnas.071543598

Roach CR, Hall DE, Zerbe P, Bohlmann J (2014) Plasticity and evolution of (+)-3-carene synthase and (-)-sabinene synthase functions of a Sitka spruce monoterpene synthase gene family associated with weevil resistance. J Biol Chem 289:23859–23869. doi: 10.1074/jbc.M114.571703

Robert JA, Madilao LL, White R, Yanchuk A, King JR, Bohlmann J (2010) Terpenoid metabolite profiling in Sitka spruce identifies association of dehydroabietic acid, (+)-3-carene, and terpinolene with resistance against white pine weevil. Botany-Botanique 88:810–820. doi: 10.1139/B10-068

Ruijter JM, Ramakers C, Hoogaars WMH, Karlen Y, Bakker O, Van Den Hoff MJB, Moorman AFM (2009) Amplification efficiency: Linking baseline and bias in the analysis of quantitative PCR data. Nucleic Acids Res. doi: 10.1093/nar/gkp045

Rynkiewicz MJ, Cane DE, Christianson DW (2001) Structure of trichodiene synthase from Fusarium sporotrichioides provides mechanistic inferences on the terpene cyclization cascade. Proc Natl Acad Sci U S A 98:13543–13548. doi: 10.1073/pnas.231313098

Sarker LS, Galata M, Demissie ZA, Mahmoud SS (2012) Molecular cloning and functional characterization of borneol dehydrogenase from the glandular trichomes of Lavandula x intermedia. Arch Biochem Biophys 528:163–70. doi: 10.1016/j.abb.2012.09.013

Van Schie CCN, Haring MA, Schuurink RC (2007) Tomato linalool synthase is induced in trichomes by jasmonic acid. Plant Mol Biol 64:251–263. doi: 10.1007/s11103-007-9149-8

Savage TJ, Croteau R (1993) Biosynthesis of monoterpenes - regiochemistry and stereochemistry of (+)-3-carene biosynthesis. Arch. Biochem. Biophys. 305, 581-587

Schilmiller AL, Schauvinhold I, Larson M, Xu R, Charbonneau AL, Schmidt A, Wilkerson C, Last RT, Pichersky E (2009) Monoterpenes in the glandular trichomes of tomato are synthesized from a neryl diphosphate precursor rather than geranyl diphosphate. Proc Natl Acad Sci U S A 106:10865–10870. doi: 10.1073/pnas.0904113106\r0904113106 [pii]

Shi J, Ma C, Qi D, Lv H, Yang T, Peng Q, Chen Z, Lin Z (2015) Transcriptional responses and flavor volatiles biosynthesis in methyl jasmonate-treated tea leaves. BMC Plant Biol 15:233. doi: 10.1186/s12870-015-0609-z

Taniguchi S, Hosokawa-Shinonaga Y, Tamaoki D, Yamada S, Akimitsu K, Gomi K (2014) Jasmonate induction of the monoterpene linalool confers resistance to rice bacterial blight and its biosynthesis is regulated by JAZ protein in rice. Plant, Cell Environ 37:451–461. doi: 10.1111/pce.12169

Tholl D, Lee S (2011) Terpene Specialized Metabolism in Arabidopsis thaliana. Arabidopsis Book 9:e0143. doi: 10.1199/tab.0143

Upson T and Andrews S (2004) The genus Lavandula (1st ed) Timber Press, Inc., USA.

De Vega C, Herrera CM, Dotterl S (2014) Floral volatiles play a key role in specialized ant pollination. Perspect Plant Ecol Evol Syst 16:32–42. doi: 10.1016/j.ppees.2013.11.002

Vickers CE, Gershenzon J, Lerdau MT, Loreto F (2009) A unified mechanism of action for volatile isoprenoids in plant abiotic stress. Nat Chem Biol 5:283–291. doi: 10.1038/nchembio.158

War A, Sharma HC, Paulraj MG, War MY, Ignacimuthu S (2011) Herbivore induced plant volatiles Their role in plant defense for pest management. Plant Signal Behav 6:1973–1978. doi: 10.4161/psb/6.12.18053

Whittington DA, Wise ML, Urbansky M, Urbansky M, Coates RM, Croteau RB, Christianson DW (2002) Bornyl diphosphate synthase: structure and strategy for carbocation manipulation by a terpenoid cyclase. Proc Natl Acad Sci U S A 99:15375–15380. doi: 10.1073/pnas.232591099

Wise M, Savage T, Katahira E (1998) Monoterpene synthases from common sage (Salvia officinalis). J Biol 273:14891–14899. doi: 10.1074/jbc.273.24.14891

Wittstock U, Gershenzon J (2002) Constitutive plant toxins and their role in defense against herbivores and pathogens. Curr Opin Plant Biol 5:300–307. doi: 10.1016/S1369-5266(02)00264-9

Xu Y-H, Liao Y-C, Zhang Z, Liu J, Sun P-W, Gao Z-H, Sui C, Wei J-H (2016) Jasmonic acid is a crucial signal transducer in heat shock induced sesquiterpene formation in Aquilaria sinensis. Sci Rep 6:21843. doi: 10.1038/srep21843

Yahyaa M, Tholl D, Cormier G, Jensen R, Simon PW, Ibdah M (2015) Identification and Characterization of Terpene Synthases Potentially Involved in the Formation of Volatile Terpenes in Carrot (Daucus carota L.) Roots. J Agric Food Chem 63:4870–4878. doi: 10.1021/acs.jafc.5b00546

Zeng G (1998) Sticky-end PCR: New method for subcloning. Biotechniques 25:206–208

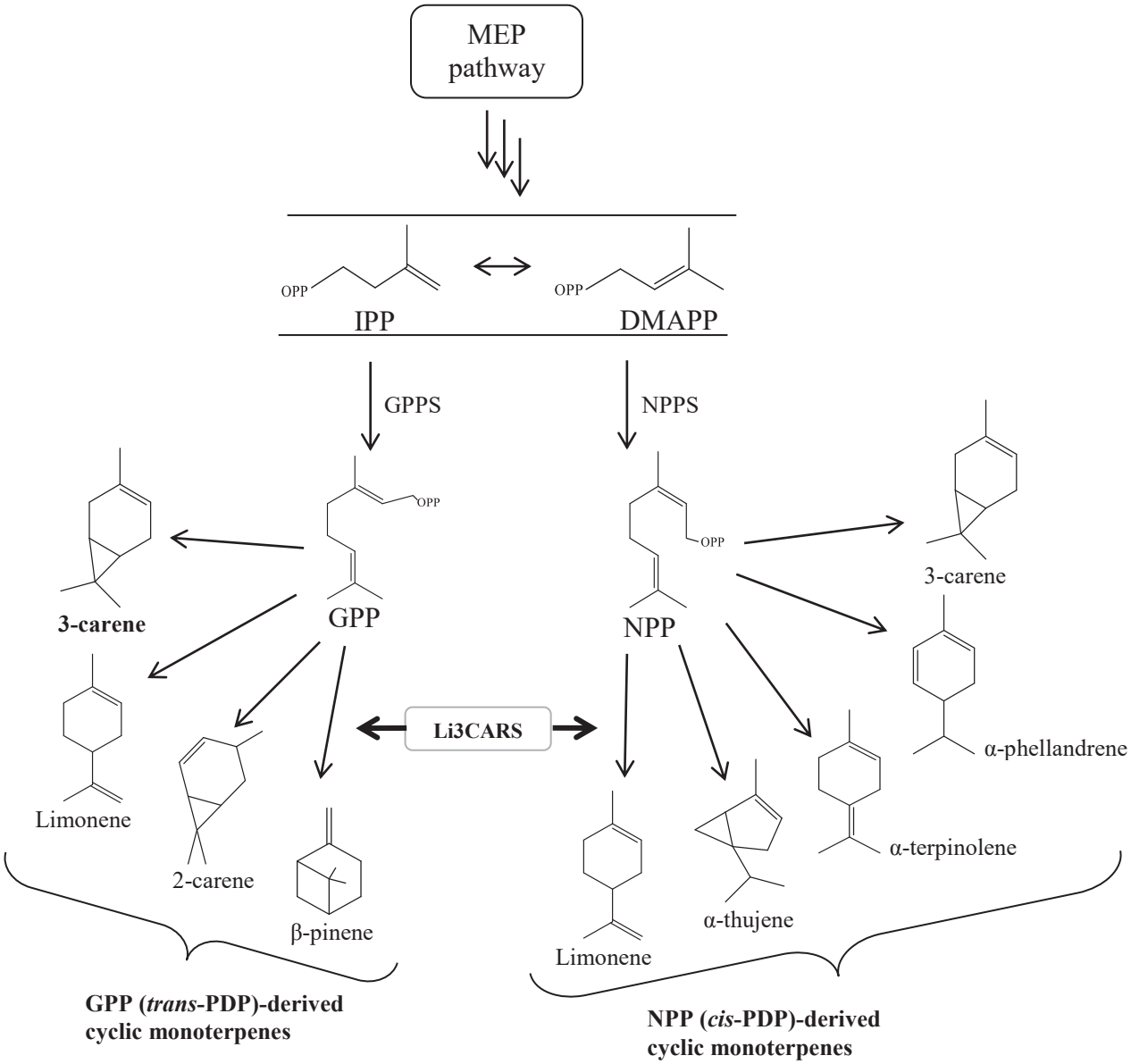
MEP pathway
OPP
IPP
OPP
DMAPP
GPPS
NPPS
OPP
3-carene
GPP
OPP
NPP
3-carene
α-phellandrene
Li3CARS
Limonene
2-carene
β-pinene
α-thujene
α-terpinolene
Limonene
GPP (trans-PDP)-derived cyclic monoterpenes
NPP (cis-PDP)-derived cyclic monoterpenes

Fig. 1.

Colour figure

Click here to download Colour figure Fig 2.docx

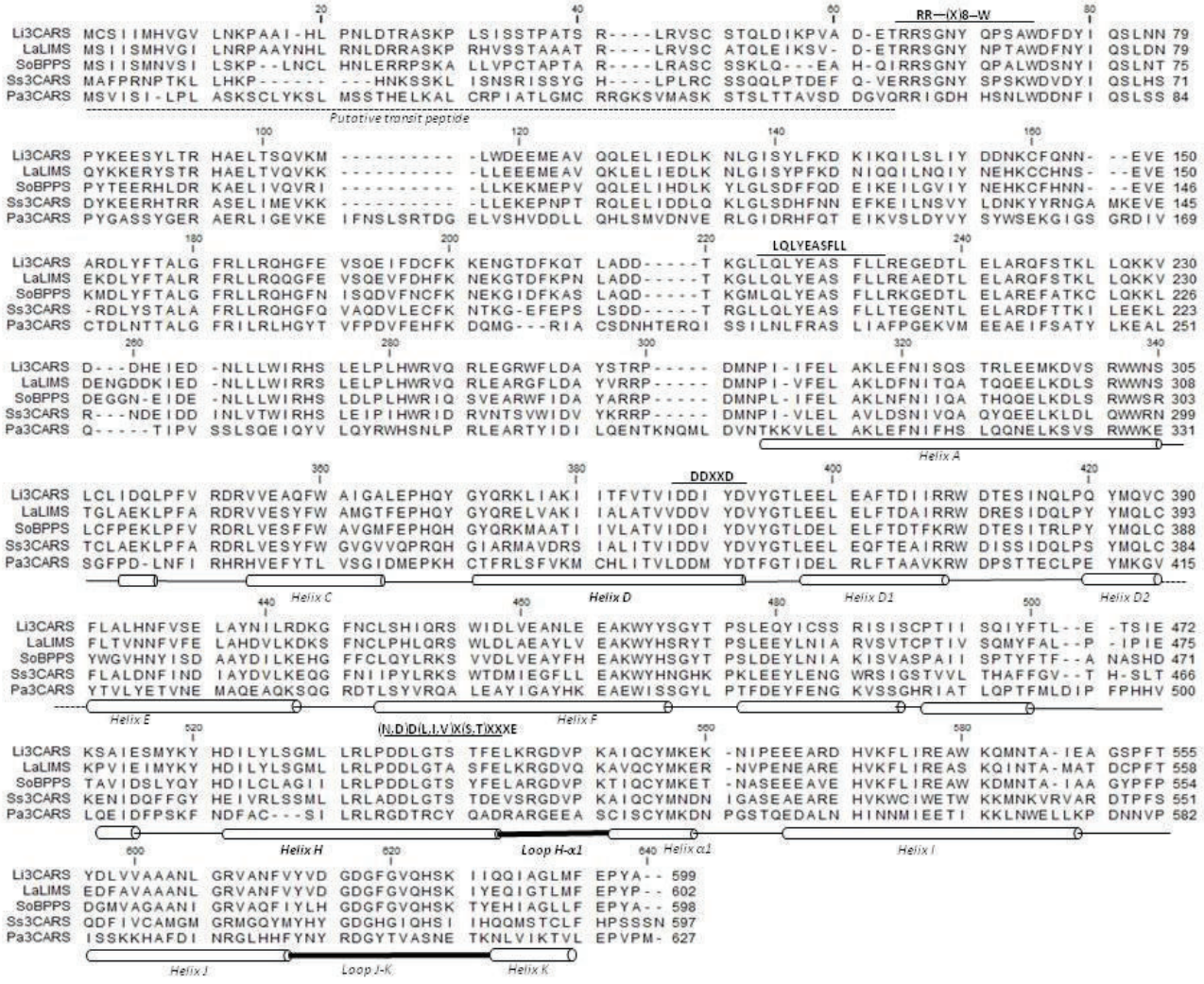

Fig. 2.

Line figure

Click here to download Line figure Fig 3.docx

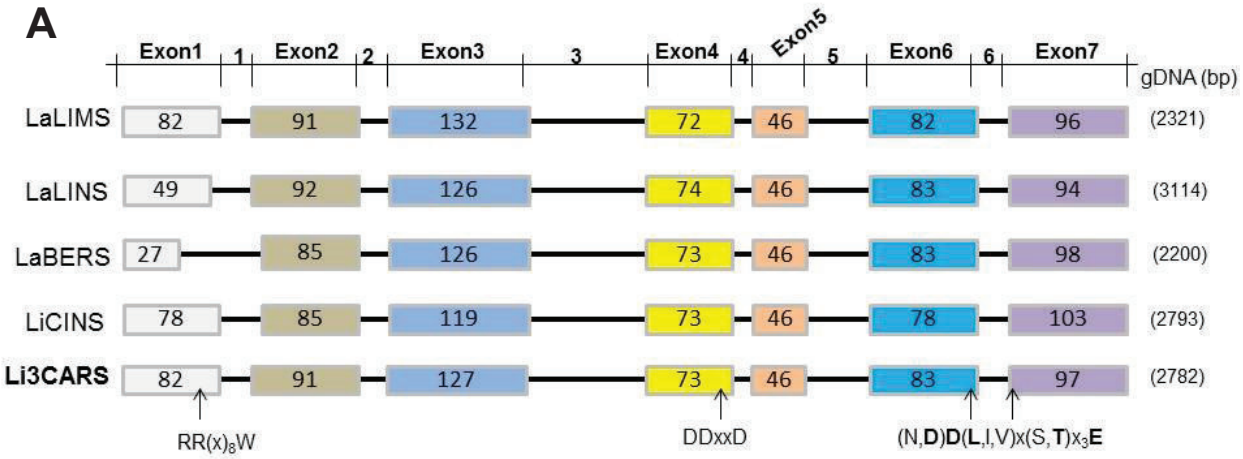

B

Gene	Intron-1	Intron-2	Intron-3	Intron-4	Intron-5	Intron-6
LaLIMS	65 bp	81 bp	105 bp	82 bp	105 bp	74 bp
LaLINS	926 bp	339 bp	93 bp	148 bp	78 bp	435 bp
LaBERS	140 bp	91 bp	79 bp	90 bp	94 bp	89 bp
LiCINS	264 bp	80 bp	155 bp	58 bp	73 bp	417 bp
Li3CARS	**71 bp**	**70 bp**	**430 bp**	**74 bp**	**225 bp**	**112 bp**

Fig. 3.

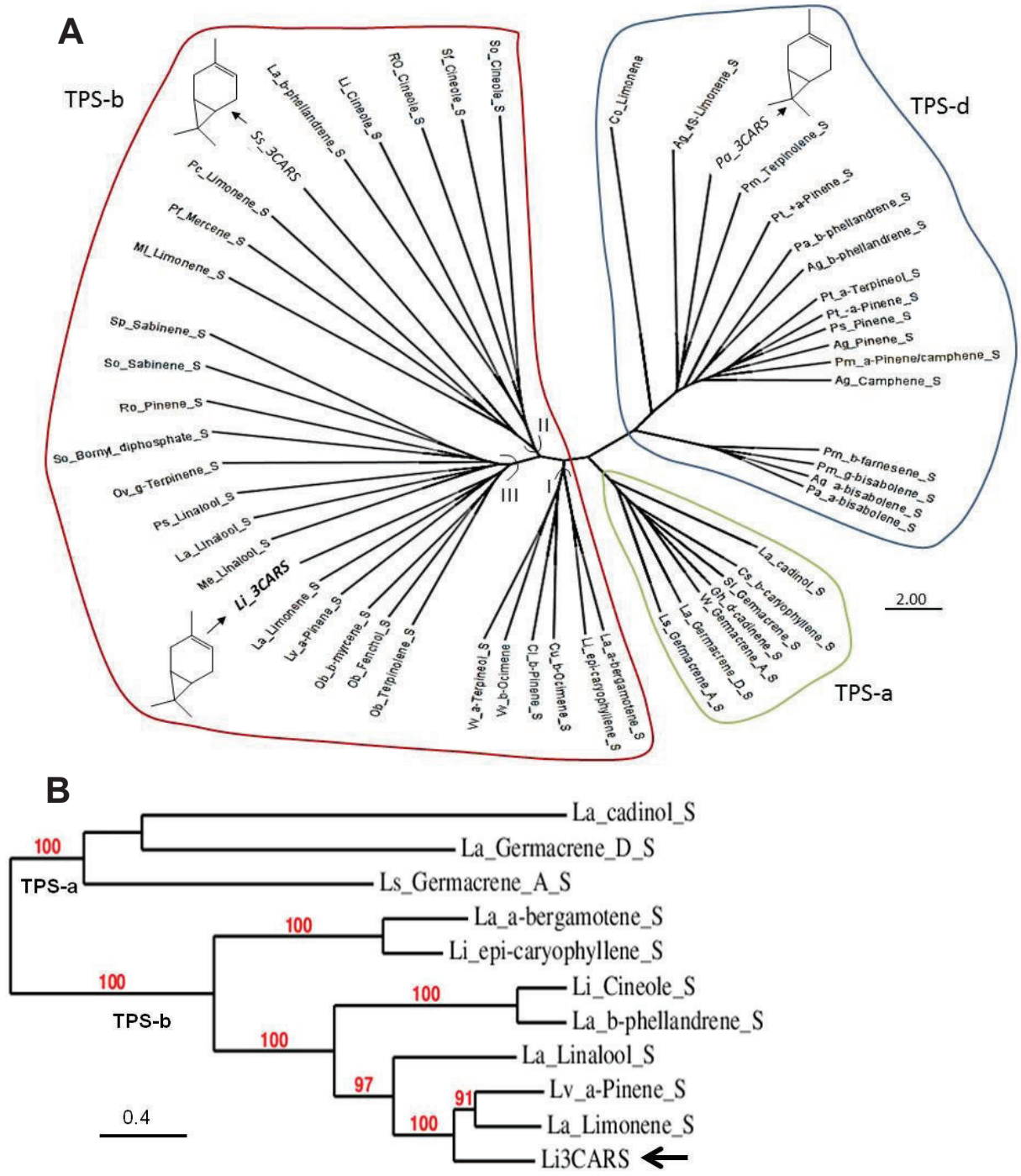
A
TPS-b
TPS-d
TPS-a
Ss_3CARS
Li_3CARS
Pd_3CARS
La_b-phellandrene_S
Li_Cineole_S
Ro_Cineole_S
St_Cineole_S
So_Cineole_S
Pc_Limonene_S
Pf_Mercene_S
Ml_Limonene_S
Sp_Sabinene_S
So_Sabinene_S
Ro_Pinene_S
So_Bornyl_diphosphate_S
Ov_g-Terpinene_S
Ps_Linalool_S
La_Linalool_S
Me_Linalool_S
La_Limonene_S
Lv_a-Pinene_S
Ob_b-myrcene_S
Ob_Fenchol_S
Ob_Terpinolene_S
Vv_a-Terpineol_S
Vv_b-Ocimene
Cl_b-Pinene_S
Cu_b-Ocimene_S
Li_epi-caryophyllene_S
La_a-bergamotene_S
Co_Limonene
Ag_4S-Limonene_S
Pm_Terpinolene_S
Pt_+a-Pinene_S
Pa_b-phellandrene_S
Ag_b-phellandrene_S
Pt_a-Terpineol_S
Pt_-a-Pinene_S
Ps_Pinene_S
Ag_Pinene_S
Pm_a-Pinene/camphene_S
Ag_Camphene_S
Pm_b-farnesene_S
Pm_g-bisabolene_S
Ag_a-bisabolene_S
Pa_a-bisabolene_S
La_cadinol_S
Cs_b-caryophyllene_S
St_Germacrene_S
Gh_d-cadinene_S
W_Germacrene_A_S
La_Germacrene_D_S
Ls_Germacrene_A_S
2.00
I
II
III
B
La_cadinol_S
La_Germacrene_D_S
Ls_Germacrene_A_S
La_a-bergamotene_S
Li_epi-caryophyllene_S
Li_Cineole_S
La_b-phellandrene_S
La_Linalool_S
Lv_a-Pinene_S
La_Limonene_S
Li3CARS
100
100
100
100
100
97
91
100
TPS-a
TPS-b
0.4

Fig. 4.

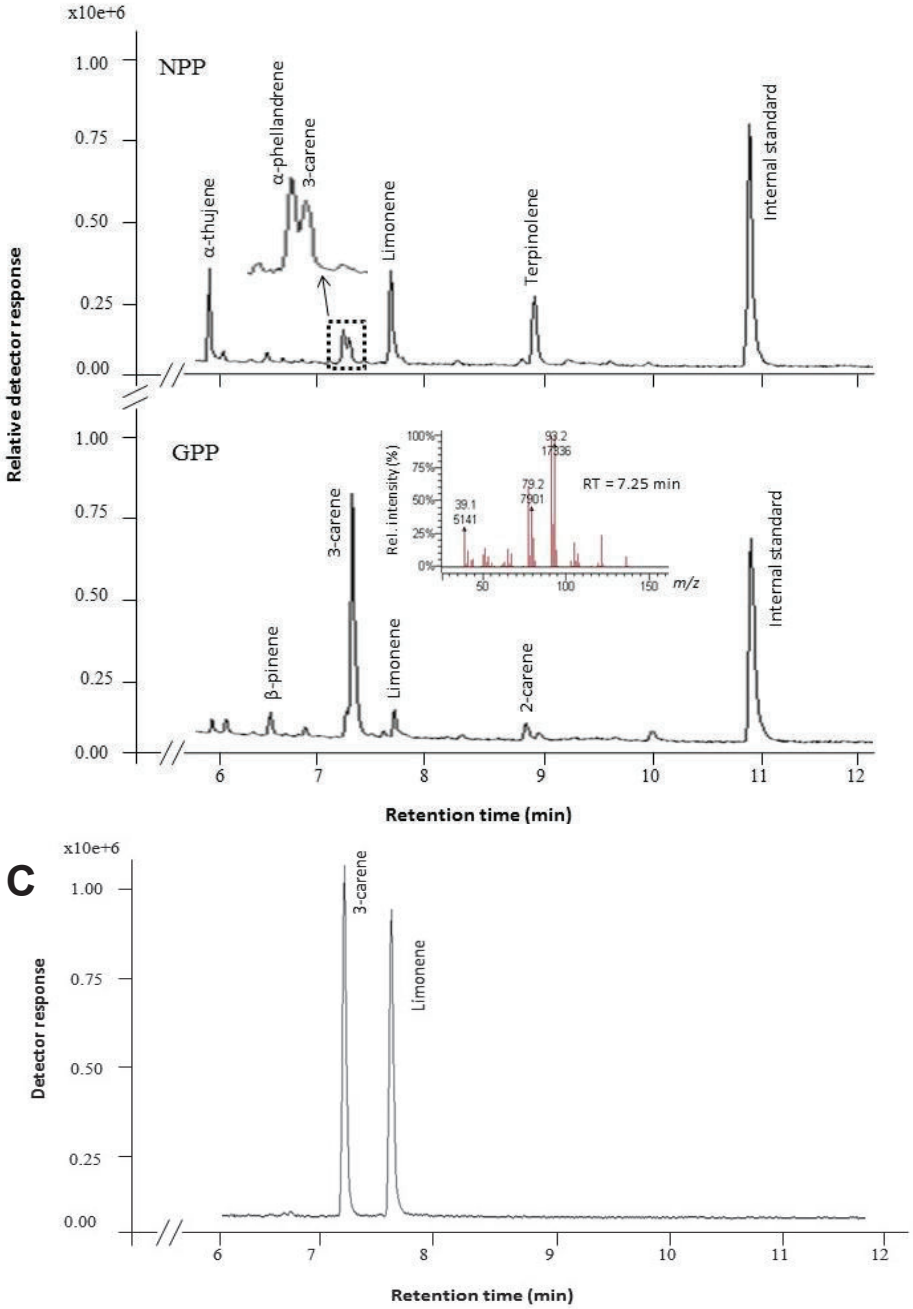
x10e+6
NPP
α-thujene
α-phellandrene
3-carene
Limonene
Terpinolene
Internal standard
GPP
β-pinene
3-carene
Limonene
2-carene
Internal standard
Rel. intensity (%)
RT = 7.25 min
93.2
17336
79.2
7901
39.1
5141
m/z
Relative detector response
Retention time (min)
C
x10e+6
3-carene
Limonene
Detector response
Retention time (min)

Fig. 5.

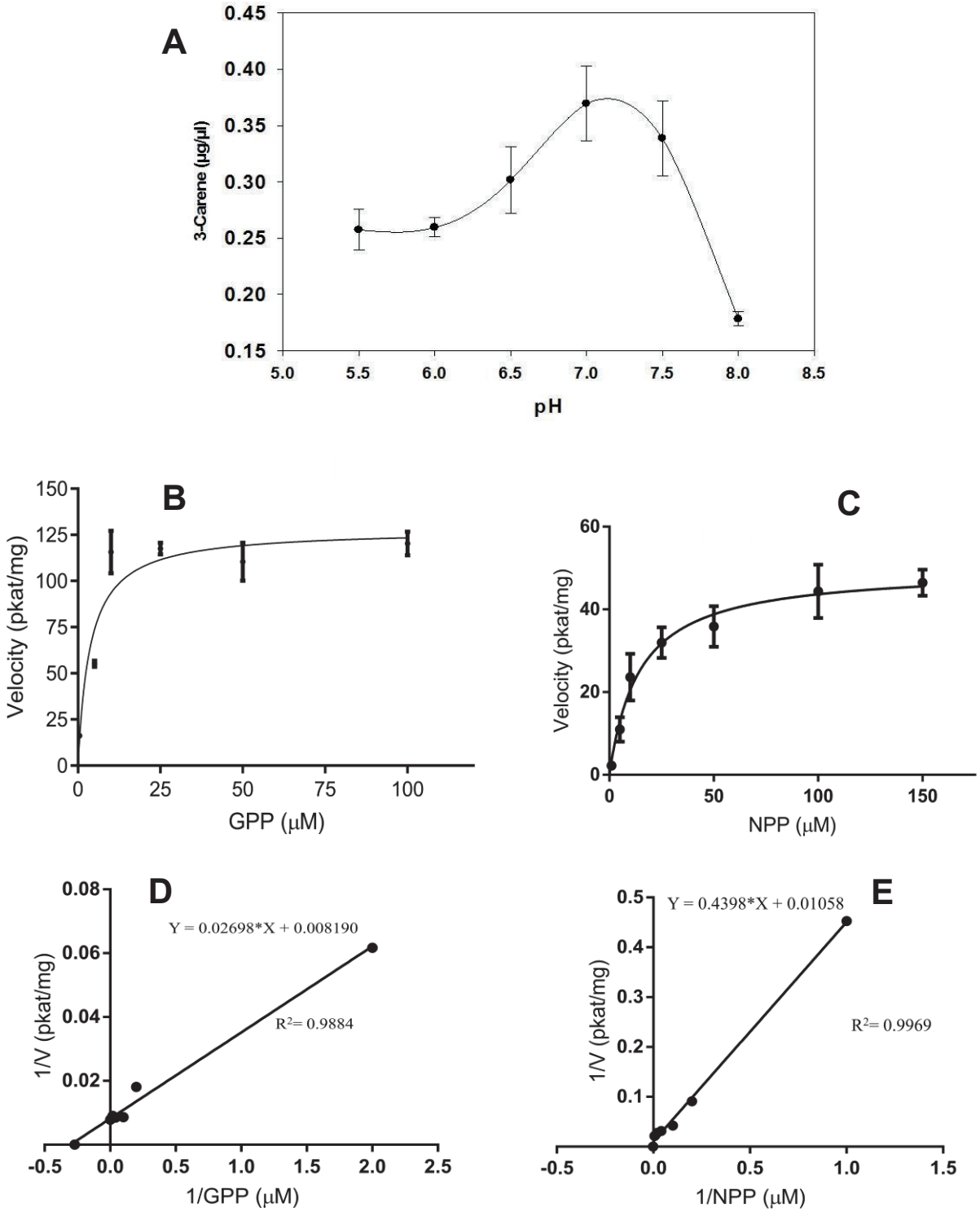

Fig. 6.

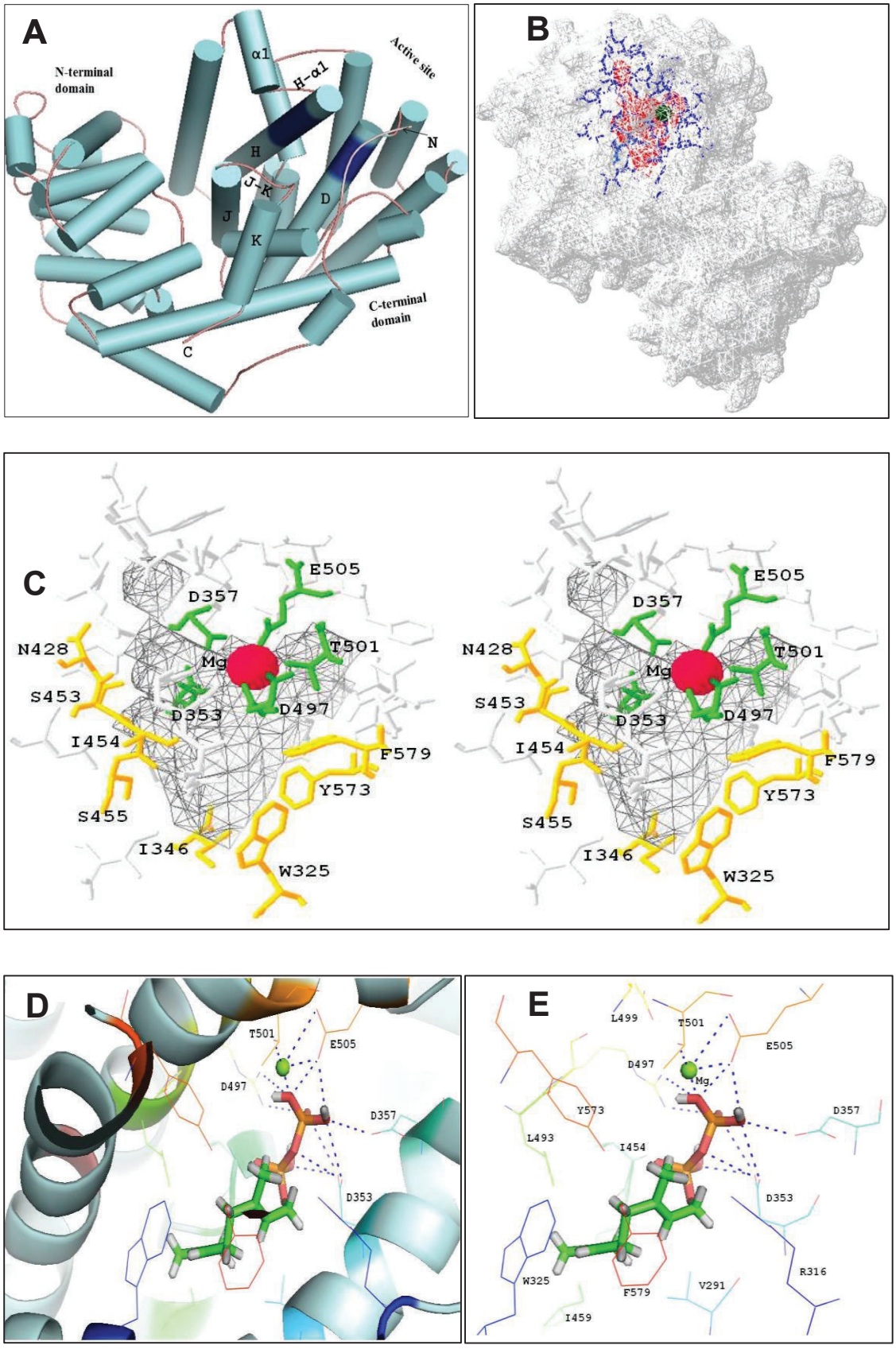
A
N-terminal domain
α1
H-α1
Active site
H
J-K
J
K
D
N
C-terminal domain
C
B
C
E505
D357
N428
T501
Mg
S453
D353
D497
I454
F579
Y573
S455
I346
W325
D
T501
E505
D497
D357
D353
E
L499
T501
E505
D497
Mg
Y573
D357
L493
I454
D353
R316
W325
F579
V291
I459

Fig. 7.

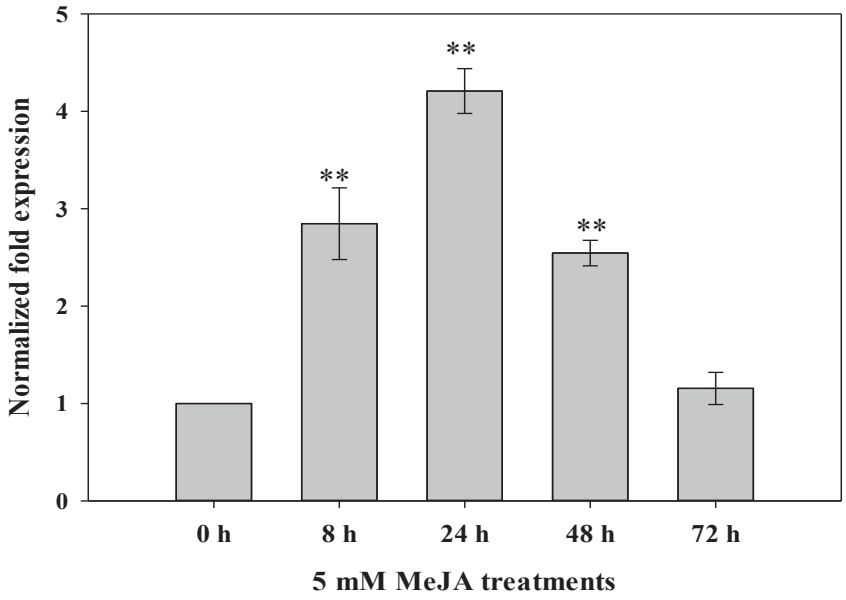

Fig. 8.

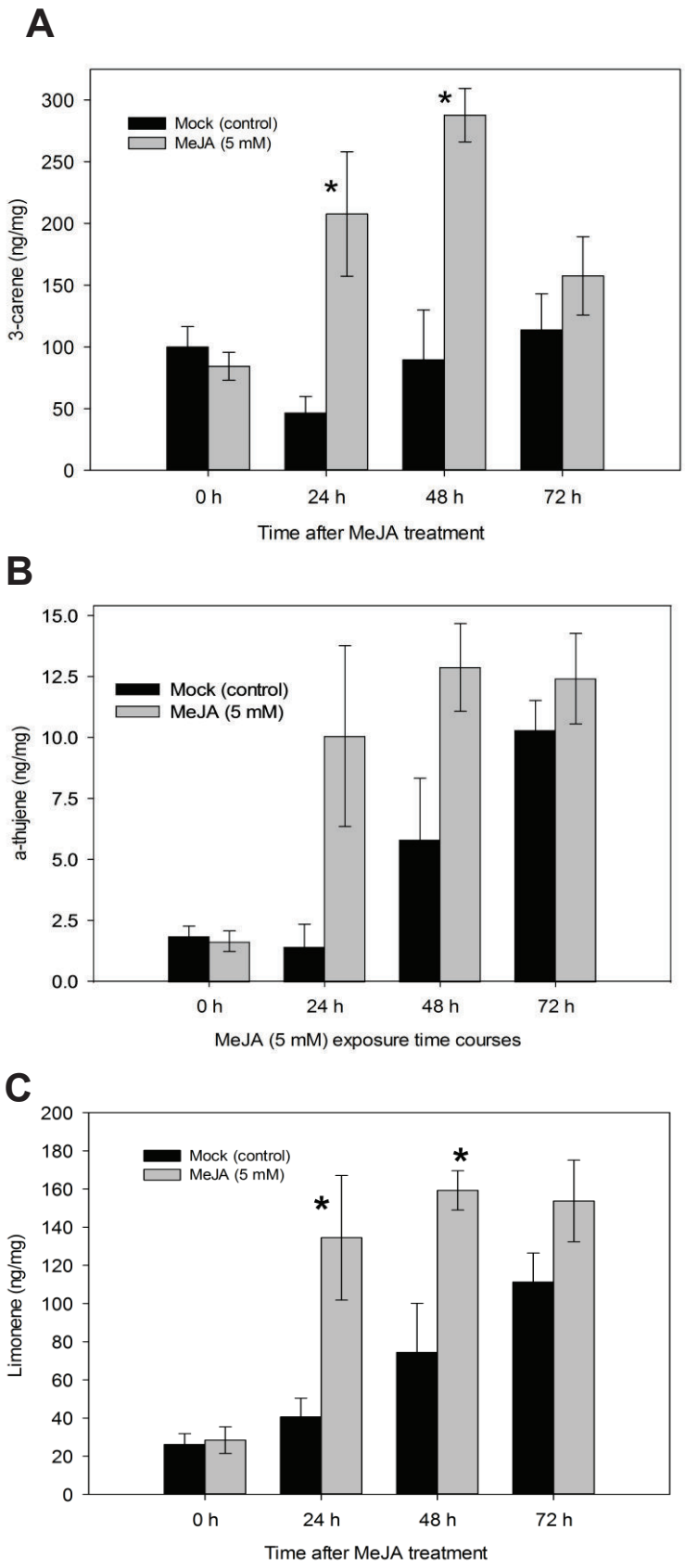

Fig. 9.

Table 1.

Gene Name	Primer name	Primer sequences (5'==> 3')	Purposes
Li3CARS cDNA	*Nde*I-Forward	CAGGAT**CATATG**TCGACACAACTAGAC	Cloning into pET41b(+) vector
	*EcoR*I-Reverse	ATTATA**GAATTC**GAAGCATACGGCTCG	
Li3CARS gDNA	Forward	ATGTGTAGCATTATCATGCATGTGG	Genomic DNA amplification
	Reverse	TATAATCTCGAGCTAAGCATACGGCTC	
Li3CARS qPCR	Forward	CCAATCAACACGGCTAGAA	qPCR quantification
	Reverse	GACCCGATCCCTTACAAATG	
β-actin	Forward	TGTGGATTGCCAAGGCAGAGT	qPCR normalization
	Reverse	AATGAGCAGGCAGCAACAGCA	
18s rRNA	Forward	GTGACGGGTGACGGAGAA	qPCR normalization
	Reverse	GACTCAATGAGCCCGGTA	

Note: underlined and bold sequences are *Nde*I and *EcoR*I restriction sites.

Table 2.

Compound name	RT	GPP	NPP
		% ± SE	% ± SE
α-Thujene	5.895	-	20.41 ± 0.27
β-Pinene	6.765	5.87 ± 0.17	-
α-Phellandrene	7.162	-	8.86 ± 0.20
3-Carene	7.257	**76.02 ± 0.54**	8.51 ± 0.15
Limonene	7.598	9. 34 ± 0.24	33.02 ± 0.22
2-Carene	8.827	8.77 ± 0.64	-
Terpinolene	8.955	-	29.20 ± 0.20

RT = retention time; SE= standard error (*n=4*)

Table 3.

Parameters	GPP	NPP			
	3-carene	**3-carene**	**α-thujene**	**limonene**	**α-terpinolene**
K_m (μM)	3.69 ± 1.17	14.3 ± 2.56	19.19 ± 3.14	23.21 ± 3.34	36.23 ± 4.33
V_{max} (pkat/mg)	128 ± 7.84	49.9 ± 2.37	105.7 ± 4.99	164.6 ± 7.27	203.5 ± 8.64
k_{cat} (s^{-1})	2.070	0.636	1.349	2.117	2.596
k_{cat}/K_m ($\mu M^{-1}s^{-1}$)	0.561	0.044	0.070	0.088	0.072